Mechanical Properties of $Ti_{50-x}Hf_xPt_{50}$, ($0 < x < 50$) for HTSMAs Applications

M P Mashamaite, H R Chauke and P E Ngoepe

Materials Modelling Centre, School of Physical and Mineral Sciences, University of Limpopo, Private Bag X1106, Sovenga 0727, South Africa

Email: mordecai.mashamaite@ul.ac.za

Abstract. Shape memory alloys (SMAs) are metallic materials that can revert to their original shape when exposed to various temperatures. These materials are used in applications such as actuators and aerospace due to their remarkable properties shape memory effect and pseudo-elasticity which occurs as a result of phase transformation. TiPt undergoes a reversible martensitic transformation from B2↔B19 at higher temperatures. Previous studies showed that the TiPt alloy is mechanically unstable with the negative C′ (–32) and soft modes in the negative frequency of the phonon dispersion curves along the gamma region at 0 K. The supercell approach was used to substitute Ti with Hf on TiPt structure to evaluate their mechanical stability from elastic properties and the phonon dispersions curves. The elastic properties suggest that an increase in Hf concentration enhances the mechanical stability of ternary systems. The C' becomes positive and larger at $25 < x < 50$, which suggests a reduced martensitic transformation at $x \geq 43.75$. The $Ti_{50-x}Hf_xPt_{50}$ systems become more ductile with the increase in Hf concentration, which suggests that Hf stabilizes the system at a higher concentration. The analyses of the vibrational properties of $Ti_{50-x}Hf_xPt_{50}$ structures with respect to phonon dispersion are also discussed.

1. Introduction

Shape memory alloys (SMAs) have found universal applications in the fields of automotive, aerospace, medicine and engineering [1]. This is due to two special properties pseudo-elasticity or super-elasticity and shape memory effect, which come as a result of phase transformation [2]. Pseudo-elasticity is an elastic response to applied stress, while the memory effect of these materials is identified with a reversible martensitic transformation (MT), which is a sort of non-diffusive structure phase change including both atomic rearrangements of positions and change in cell volume [3]. In this effect, the study of phase stability has been an interesting subject [4]. The main SMAs available are those dependent on NiTi composites, which are utilized in medical industries for dental gadgets, stents, bone plates, eyeglass casings, and in robotics where the application temperature doesn't surpass 373K [5]. NiTi keeps on overwhelming the developing business sector due to their attractive mechanical properties in their capacity to accomplish functionality when compared with different SMAs, great corrosion resistance and biocompatibility [6].

There exists a mounting need today for even unrivalled SMAs, the journey for which is likewise going through quick development [7]. However, huge advancement has been made in expanding the reach that NiTi-based alloys can be used in actuator-based applications through ternary alloying [8]. A

few alloying additions, for example, Au, Pd, Pt, Zr and Hf, have appeared to build the martensitic transformation temperatures answerable for the shape memory attributes of NiTi SMAs [9]. Some of these ternary alloys were successfully reported to have increased the transformation temperature of NiTi [10]. High temperature shape memory alloys (HTSMAs) are costly and are still under investigation due to their great functionality and high martensitic transformation temperatures of up to 800 K. However, the most attention was focused on Ni-Ti–Zr, and Ni-Ti–Hf HTSMAs mainly due to the generally low costs for crude materials as compared with the Nobel metals (Au, Pd, and Pt) [11].

Possible elective systems for NiTi can be TiPd and TiPt. TiPd undergoes a B2 to B19 martensite phase transformation with a martensite start temperature (Ms) between 783 and 836 K [12]. Moreover, equiatomic TiPt exhibits martensitic transformation temperature much higher than NiTi and its ternaries above 1200 K [13]. Various reports have demonstrated that TiPt alloy exhibited negligible shape memory effect (11%), due to the low critical stress for slip deformation compared to the stress required for martensitic reorientation [14]. Newer SMAs systems are being developed for extremely high temperature applications. Investigations of ternary shape memory alloys dependent on TiPd have been growing rapidly, studies on Ti–Pd–M, where M = (Ni, Pt, Ir, Co and Ru) alloys show high work output and good workability [15]. Ru was found to be effective in hardening and increasing resistance to heat and corrosion [16]. For this reason, TiPt and its ternary have been investigated to improve its mechanical workability [17].

Equiatomic TiPt is even more promising as a very HTMSA since it is reported to undergo a B2 to B19 martensite phase transformation with a Ms of approximately 1323 K [18]. However, TiPt based alloys have their drawbacks which limit their possible usage, upon the improvement of shape memory properties, the alloy could be used for various temperature applications [19, 20].

In this work, Hf was selected as the third element to improve the properties of the B2 TiPt, particularly because Hf has a greater atomic radius and melting point than both Ti and Pt. First-principle method was used to investigate the effect of Hf on equiatomic TiPt, utilizing thermodynamic and mechanical properties (elastic and phonon dispersion curves).

2. Methodology

The first-principles calculations were performed using density functional theory (DFT) formalism as incorporated with a plane-wave basis in the Vienna *ab initio* Simulation Package (VASP) [21, 22]. The projector augmented wave (PAW) was used to treat core-electron interaction [23]. The exchange-correlation functional generalized gradient approximation (GGA) of the Perdew-Burke-Ernzerhof (PBE) [24] was chosen. The plane wave cut–off energy was set at 500 eV to converge the total energy of the binary TiPt alloys. The geometry optimization and the energy were carried out using a *k*-spacing of 0.25 equivalent to the *k*-point mesh of 8×8×8 according to Monkhorst and Pack [25]. A 2×2×2 supercell of TiPt was employed to substitute Ti with Hf. In the elastic constant calculations, a strain of 0.005 was used for $Ti_{50-x}Hf_xPt_{50}$ systems. The PHONON code was used to investigate the phonon dispersion spectra and the phono Density of State (phonon DOS). The phonon scatterings for the structures were determined in the system of the direct technique, for which the force constants were inferred by a supercell approach [26].

3. Results and Discussion

3.1. Lattice parameter and heats of formation

Figure 1 present the change in (a) lattice parameter and (b) heats of formation against composition of $Ti_{50-x}Hf_xPt_{50}$ where, $0 < x < 50$. The calculated lattice parameters of the $Ti_{50-x}Hf_xPt_{50}$ are shown in Figure 1 (a). The current findings show that the lattice parameter increases with an increase in Hf content. This is due to the large atomic radius of Hf (0.155nm) as compared to both Ti (0.140nm) and Pt (0.135nm). The binary $Ti_{50}Pt_{50}$ gave an equilibrium lattice parameter and the lowest value of a = 3.180 Å after optimization, which is in agreement with experimental findings of 3.192 Å [18] followed by $Hf_{6.25}Ti_{43.75}Pt_{50}$ with the value a = 3.196 Å. It is also observed the lattice parameter that the volume ($Å^3$) increases with an increase in Hf content.

The heats of formation (ΔH_f) of the intermetallic systems can be calculated from the following equation [27]:

$$\Delta H_f = E_{TiPtHf} - \sum_i x_i E_i, \quad (1)$$

where E_{TiPtHf} total energy of an intermetallic system, and E_i is the total energy of the individual elements in the system.

The calculated heats of formation (ΔH_f) in Figure 1 (b) show that TiPt becomes stable with an increase in Hf content. $Hf_{50}Pt_{50}$ is the most thermodynamically stable structure, and the most stable ternary being $Hf_{43.75}Ti_{6.25}Pt_{50}$ (- 0.966 eV/atom).

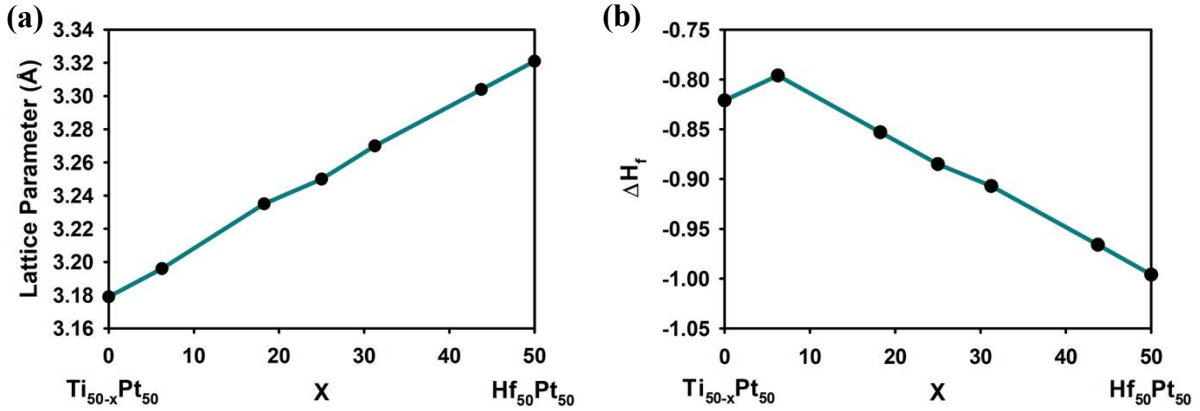

Figure 1. Change in (a) Lattice parameter and (b) Heats of formation (ΔH_f) against composition $Ti_{50-x}Hf_xPt_{50}$, $0 < x < 50$

3.2. Elastic constants

Elastic constants are vital material parameters, the investigation of elastic constants gives a connection between the mechanical properties and dynamic data concerning the idea of the forces working in solids, particularly for the solidness and stiffness of materials. Brittleness (B), ductility, stiffness, stability, and anisotropy (*A*) of material are some of the key fundamental solid-state phenomena of elastic constants. Since the intermetallic compound TiPt belongs to the cubic crystal, it has three independent elastic constants C_{11}, C_{12} and C_{44}. This system has been adequately used to consider the elastic properties of various metallic structures [28].

For a cubic system, the mechanical stability conditions are given by [29].

$$C_{11}, C_{44}, C_{11} > |C_{12}| \text{ and } C_{11} + 2C_{12} > 0, \quad (2)$$

The elastic constants were evaluated to observe the effect of 0.005 strain when substituting Ti with Hf. All the independent elastic constants C_{11}, C_{12}, and C_{44} for $Ti_{50-x}Hf_xPt_{50}$ were positive which indicates the mechanical stability of the system. The $C_{11} < C_{12}$ from 6.25 – 18.75 at.% which gives a negative C'. Furthermore, $C_{11} > C_{12}$ from 25 – 43.75 at.% contributes to a positive C'. The positive C' suggests that the ternary at 25 – 43.75 at.% Hf, the compositions satisfy the stability conditions. The C' increases with the addition of Hf to the system, it is also observed that positive and larger C' leads to $A > 1$. Elastic anisotropy of crystals is significant since it associates with the possibility to instigate miniature breaks in materials. The anisotropy factor is the proportion of the level of anisotropy in solid materials [30]. For a completely isotropic material $A = 1$, whereas the degree of elastic anisotropy is $A > 1$ or $A < 1$. As shown in Table 1, the value of A for $x > 25$ is greater than 1, which indicates that the ternaries can be regarded as an elastically anisotropic material. The martensitic transformation temperature of $Ti_{50-x}Pt_{50}$ is lowered with an increase in Hf up to 43.75 at. %, which is due to C'. Contrary to the rise in martensitic transformation at Hf 6.25 at. % due to low C'.

Table **1**. The elastic constants C_{ij} (GPa), shear moduli C' and anisotropy A for $Ti_{50-x}Hf_xPt_{50}$, $0 < x < 50$.

Structure	C_{11} **(GPa)**	C_{12} **(GPa)**	C_{44} **(GPa)**	C'	A
$Ti_{50}Pt_{50}$	145	210	45	-32.5	-1.38
$Hf_{6.25}Ti_{43.75}Pt_{50}$	105	229	54	-62	-0.87
$Hf_{18.75}Ti_{31.25}Pt_{50}$	147	206	47	-30	-1.59
$Hf_{25}Ti_{25}Pt_{50}$	192	187	40	2.5	16
$Hf_{31.25}Ti_{18.75}Pt_{50}$	202	178	46	12	3.83
$Hf_{43.75}Ti_{6.25}Pt_{50}$	209	173	44	18	2.44
$Hf_{50}Pt_{50}$	209	172	43	19	2.32

Another index to describe the brittleness or ductility of a system is Pugh's ratio which is defined as $k = B/G$, the B/G ratio must be > 1.75 for the material to be regarded as ductile, if < 1.75 then the material is brittle [31]. In Figure 2 (a), the structures displayed ductility with an increase in Hf content, since B/G >1.75. The dip at 18. 25 at.% of Hf was caused by lower values of G. Furthermore, 6.25 at.% Hf is brittle with k = 1.68.

Cauchy pressure can be portrayed as $C_{12} - C_{44}$, which may be utilized to portray the angular character of atomic bonding in different metals and compounds. The negative estimation of Cauchy pressure demonstrates that the material is non-metallic with directional bonding and while for positive estimation of the material; it is required to be metallic. [32]. From Figure 3 (b), it is evident that the values of $C_{12} - C_{44}$ of $Ti_{50-x}Hf_xPt_{50}$ are positive, which indicates the metallic behavior of the compound. Furthermore, according to $C_{12} - C_{44}$, it is noticeable that the metallic behavior of $Ti_{50-x}Hf_xPt_{50}$ is getting weaker with an increase in Hf content. Therefore, the $Ti_{50-x}Hf_xPt_{50}$ maintained a metallic behavior as Hf is introduced to the system.

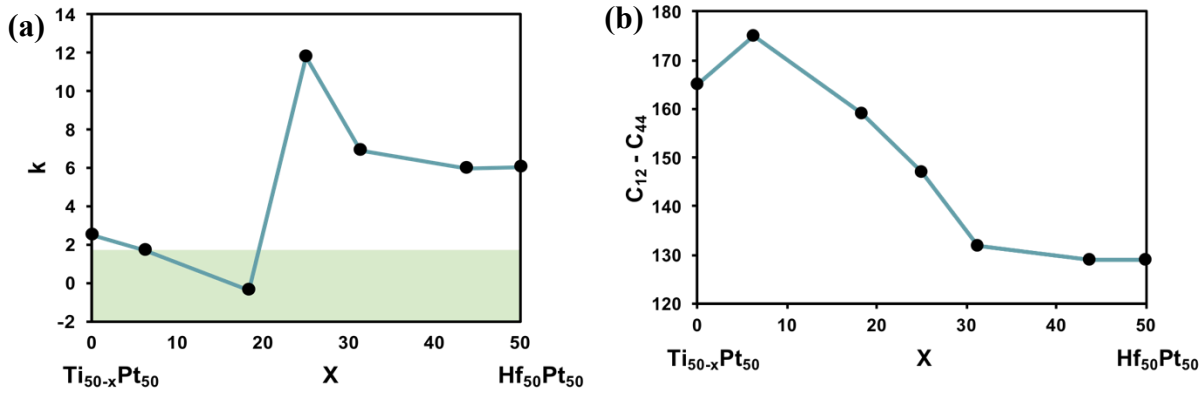

Figure 2. (a) Pugh's ratio k and (b) Cauchy pressure against composition $Ti_{50-x}Hf_xPt_{50}$, $0 < x < 50$

3.3. Thermal properties

It is imperative to appreciate the Debye temperature, chemical bonds, and the mechanical solidness of materials. The Debye temperature (Θ_D) is firmly identified with numerous actual properties, for example, versatile consistent, explicit warmth and melting point and it can be assessed through the mean sound speed utilizing the accompanying condition [33, 34].

$$\theta_D = \frac{h}{k_B}\left(\frac{3n}{4\pi\Omega}\right)^{1/3} \times v_m, \quad (3)$$

where h is the Planck constant, n is the number of atoms in the unit cell. The average sound velocity in a system, v_m is given by [35]:

$$v_m = \left[\frac{1}{3}\left(\frac{2}{v_t^3} + \frac{1}{v_l^3}\right)\right]^{-1/3}, \quad (4)$$

where v_t and v_l are the transverse and longitudinal elastic wave velocities, respectively, which can be written as:

$$v_t = \left(\frac{G}{\rho}\right)^{1/2} \text{ and } v_l = \left(\frac{3B+4G}{3\rho}\right)^{1/2}. \quad (5)$$

The calculated Debye temperature of the $Ti_{50-x}Hf_xPt_{50}$ compositions is summarized in Table 2. The density of the TiPt increases with an increase in Hf, this is deducted from the lattice parameter in section 3.1. The Θ_D can also be used to describe the strength of covalent bonds in solid materials [36]. The obtained results indicate that the covalent bonds in $Hf_{6.25}Ti_{43.75}Pt_{50}$ are greater than all other compositions. The Debye temperature increases in the sequence $Hf_{18.75}Ti_{31.25}Pt_{50} < Hf_{25}Ti_{25}Pt_{50} < Hf_{50}Pt_{50} < Hf_{31.25}Ti_{18.75}Pt_{50} < Hf_{43.75}Ti_{6.25}Pt_{50} < Ti_{50}Pt_{50} < Hf_{6.25}Ti_{43.75}Pt_{50}$.

Table 2. The density ρ (Mg/m_3), transverse v_t, longitudinal v_l and mean elastic wave velocity v_m (m/s) and Debye temperature Θ_D (K) for $Ti_{50-x}Hf_xPt_{50}$, $0 < x < 50$.

Composition	ρ	v_t	v_l	v_m	Θ_D
$Ti_{50}Pt_{50}$	12.614	2553	4854	2855	337
$Hf_{6.25}Ti_{43.75}Pt_{50}$	12.614	2916	5054	3237	380
$Hf_{18.75}Ti_{31.25}Pt_{50}$	13.210	871	3728	995	115
$Hf_{25}Ti_{25}Pt_{50}$	14.324	1026	3746	1171	135
$Hf_{31.25}Ti_{18.75}Pt_{50}$	14.917	1329	3799	1511	173
$Hf_{43.75}Ti_{6.25}Pt_{50}$	15.411	1372	3709	1557	177
$Hf_{50}Pt_{50}$	16.441	1343	3647	1525	172

3.4. Phonon dispersion curves

The scattering relations display two kinds of phonons in particular the optical and acoustic modes corresponding to the upper and lower sets of bends in the chart, respectively.

The analyses of the vibrational properties concerning the phonon dispersion curves and the phonon DOS of the $Ti_{50-x}Hf_xPt_{50}$ (x = 6.25, 18.75, 25, 31.25 and 43.75) are shown in Figure 3. Previous reports show that the B2 TiPt has soft modes due to Pt contribution and while Ti contributes to the acoustic mode in the positive direction [37], In addition, on Pt substitution with Hf, $Ti_{50}Pt_{31.25}Hf_{18.75}$ and $Ti_{50}Pt_{25}Hf_{25}$ were found to be vibrational stable due to the absence of soft modes in the negative direction of phonon dispersion curves [38]. Interestingly, From Figure 3, it is observed that the soft mode along all the high symmetry directions has the lowest frequency at approximately -3THz and a slight shift in the acoustic region since Ti was substituted with Hf. The phonon dispersion curves are highly unstable due to the presence of soft modes along with the high symmetry directions. A similar trend is observed in all compositions. The phonon DOS of the $Ti_{50-x}Hf_xPt_{50}$ x = 6.25, 18.75, 25, 31.25 and 43.75 is plotted on each right side of the phonon spectra. The Phonon DOS shift minimally with an increase in Hf content. This is due to the high Pt content in the ternary system. The Pt element contributes more towards the soft modes in the negative direction [38]. In addition, from all the concentrations below the Pt atoms vibrate at lower frequencies, while on the contrary, Ti atoms vibrate towards higher frequencies.

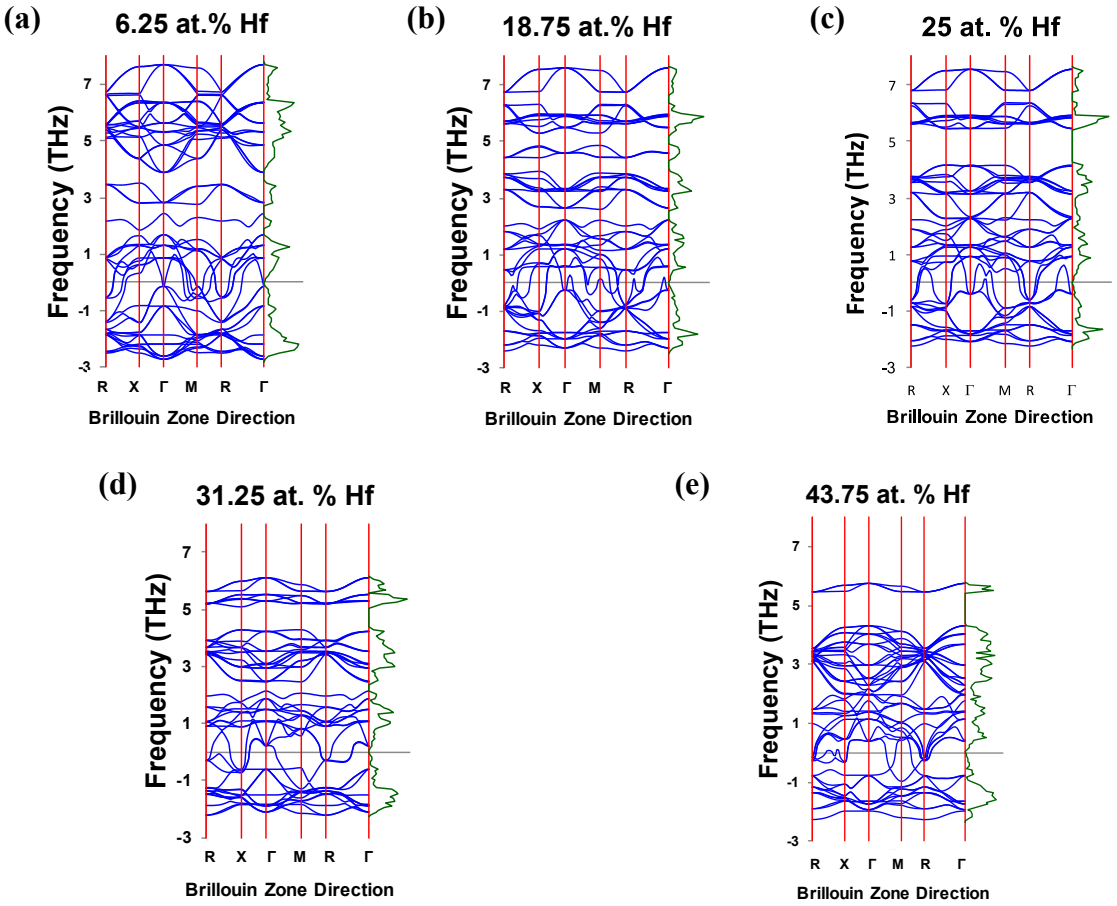

Figure 3. Phonon dispersion curves and phonon DOS for $Ti_{50-x}Hf_xPt_{50}$, $0 < x < 50$

4. Conclusions

First-principle was used to investigate the structural, thermodynamic and mechanical properties in $Ti_{50-x}Hf_xPt_{50}$ where $0 < x < 50$. The lattice parameter behaviour depends on the type of the third element, atomic radius, density and sub-lattice. The addition of Hf displayed an increase in lattice parameters due to the atomic radii and densities. Thermodynamic stability for the ternary system was investigated by partially substituting some of the Ti with Hf, it was observed that Hf (-0.966 eV/atom) at 43.75 at.% the substitutions were the most stable structures. The C_{44} decreases slightly which leads to an increase in transformation temperature. The C′ shear resistance of the $Ti_{50-x}Hf_xPt_{50}$ compound is raised with the increase in Hf content, which leads to positive and larger anisotropy. Cauchy pressure confirmed metallic behavior of the $Ti_{50-x}Hf_xPt_{50}$ ($0 < x < 50$) systems. The calculated structures show good thermal conductivity as deduced by the Debye temperature. The phonon dispersion curves were also calculated and suggest that the addition of Hf needs more strain to stabilize TiPt at compositions greater than 6.25at. % or some substitution to Pt sub-lattice.

Acknowledgements

This research was supported by MMC at the University of Limpopo and the CHPC. M. P Mashamaite, H. R Chauke and P. E Ngoepe also acknowledge the TiCoC the financial support.

References

[1] Zhao G L and Harmon B N 1993 *Phys. Rev. B* **48** 2031
[2] Jani J M, Leary M , Subi A and Gibson M A 2014 *Mater. Des.* **56** 1078
[3] Majid T, Vijay G and Mohammad H E 2012 *J. Med. Devices* **6** 034501
[4] Cai J, Wang D S, Liu S J, Duan S Q and Ma B K 1999 *Phys. Rev. B* **23** 15691
[5] Otsuka K and Ren X 2005 *Prog. Mater Sci.* **50** 511
[6] Morgan N B 2004 *Mater. Sci. Eng. A* **378** 16
[7] Chowdhury P 2018 *Shap. Mem. Superelasticity* **4** 26
[8] Bozzolo G, Mosca H O and Noebe R D 2007 *Intermetallics* **15** 901
[9] Firstov G S, Van Humbeeck J and Koval Y N 2004 *Mater. Sci. Eng. A* **378** 2
[10] Suzuki Y, Xu Y, Morito S, Otsuka K and Mitose K 1998 *Mater. Lett.* **36** 85
[11] Ma J, Karaman I and Noebe R 2010 *Int. Mater. Rev.* **55** 257
[12] Cai W, Tanaka S, Otsuka K 2000 *Mater. Sci. Forum* **279** 327
[13] Kawamura T, Tachi R, Inamura T, Hosoda H, Wakashima K, Hamada K and Miyazaki S 2006 *Mater. Sci. Eng.* **A438** 383
[14] Yamabe-Mitarai Y, Hara T, Miura S and Hosoda H 2010 *Intermetallics* **18** 2275
[15] Kumar P K, Lagoudas D C, Zanca J, and Lagouda M Z 2006 *Proc. of SPIE* **12** 6170
[16] Hamond C R 2005 *The elements. Boca Raton, FL: CRC*
[17] Mashamaite M P, Chauke H R and Ngoepe P E 2019 *IOP Conf. Ser.: Mater. Sci. Eng*. **655** 012011
[18] Donkersloot H C and van Vucht J H N 1970 *J. Less-Common Metals*. **20** 83
[19] Yamabe-Mitarai Y, Hara T, Miura S, Hosoda H 2006 *Mater. Trans.* **47** 650
[20] Wadood A, Takahashi M, Takahashi S, Hosoda H and Yamabe-Mitarai Y 2013 *Mater. Sci. Eng.* **A564** 34
[21] Hohenberg P and Kohn W 1964 *Phys. Rev. B.* **136** 864
[22] Kohn W and Sham L J 1965 *Phys. Rev* **140** A1133
[23] Blöchl P E 1994 *Phys. Rev. B.* **50** 17953
[24] Perdew J P, Burke K and Ernzerhof M 1996 *Phys. Rev. Lett.* **77** 3865
[25] Monkhorst H J and Pack J D 1976 *Phys. Rev. B.* **13** 5188
[26] Parlinski K, Li Z Q and Kawazoe Y 1997 *Phys. Rev. Lett*. **78** 4063
[27] Fernando G W, Watson R E and Weinert M 1992 *Phys. Rev. B* **45** 15 8233
[28] Zhang J M and Guo G Y 1997 *Phys. Rev. Letters* **78** 4789
[29] Mehl M J and Klein B M 1994 *Inter. Comp.* **1** 1
[30] Goumri-Said S and Kanoun M B 2007 *Comp. Mat. Sci.* **43** 243
[31] Pugh S F 1954 Philos. Mag. **45** 823
[32] Pettiifor D G 1992 J. Mater. Sci. and Tech. **8** 345
[33] Ghebouli B, Ghebouli M, Bouhemadou M, Fatmi M, Khenata R, Rached D, Ouahrani, Omran S B 2012 *Solid State Sci.* **14** 903
[34] Bouhemadou A 2009 Solid State Sci. **11** 1875
[35] Hao X, Xu Y, Wu Z, Zhou D, Liu X, Cao X, Meng J 2006 *Phys. Rev. B: Condens. Matter* **74** 224112
[36] Huang Z W, Zhao Y H, Hou H, Han P D 2012 *Phys. B* (2012) **407** 1075
[37] Mahlangu R, Phasha M J, Chauke H R, Ngoepe P E 2013 *Intermetallics,* **3** 31
[38] Baloyi M E, Modiba R, Ngoepe P E and Chauke H R 2019 *SAIP Proceedings* 18